

# ***In vitro* phototoxicity and dark-toxicity of a novel synthesized pyropheophorbide-a-paclitaxel conjugate against cancer cell lines**

**Gantumur Battogtokh<sup>a</sup>, Hai-Bo Liu<sup>a</sup>, Su-Mi Bae<sup>a</sup>, Pankaj K. Chaturvedi<sup>a</sup>, Yong-Wan Kim<sup>a</sup>, In-Wook Kim<sup>a</sup> and Woong Shick Ahn<sup>\*a,b</sup>**

<sup>a</sup> *Cancer Research Institute, Catholic Research Institute of Medical Science, The Catholic University of Korea, 505 Banpo-dong, Seocho-gu, Seoul 137-701, Republic of Korea*

<sup>b</sup> *Department of Obstetrics and Gynecology, College of Medicine, The Catholic University of Korea, 505 Banpo-dong, Seocho-gu, Seoul 137-701, Republic of Korea*

**ABSTRACT:** Synthesis of pyropheophorbide-a-paclitaxel (PPa-PTX) conjugate was performed in high yield with the aim of searching for an optimal agent for cancer treatment. After synthesis, the conjugate was confirmed to be linked through an ester bond at the 2' position of the paclitaxel moiety using multinuclear magnetic resonance spectroscopy. Phototoxicity of PPa and PPa-PTX conjugate, as well as PTX, was evaluated with three human cancer cell lines (HeLa, CaSki and TC-1). The new conjugate at 0.01–0.06  $\mu\text{M}$  displayed 20–40% higher phototoxicity in HeLa and CaSki cell lines than free PPa and PTX. Furthermore, cellular uptake of these bio-molecules was examined by confocal laser scanning microscopy. Although PPa-PTX showed a delayed uptake compared to PPa, it penetrated completely into cells within 24 h incubation.

**KEYWORDS:** pyropheophorbide-a, paclitaxel, PDT, photosensitizer, phototoxicity, synthesis.

## **INTRODUCTION**

Photodynamic therapy (PDT) is a promising approach for cancer treatment. PDT involves a combination of photosensitizer (PS) with a light in an oxygen rich environment [1, 2]. The advantage of PDT comes out preferential uptake of PS by the malignant tissue and the ability of PS to destroy a specific region when irradiation is supplied [3]. PSs used in PDT are most often derived from tetrapyrrolic compounds such as porphyrins, chlorins, phthalocyanines, texaphyrins, and bacteriochlorins [4–6]. Of these PSs, chlorin and bacteriochlorin derivatives meet the majority of the requirements for an ideal PDT PS [7–10]. However, there are challenges to improve their properties for further development of PDT [11].

Paclitaxel (PTX), a complex taxane diterpene, was originally isolated from *Taxus brevifolia*, which is one of the most effective and widely-used antitumor drugs

in cancer chemotherapy [12–14]. It has been approved for use in the United States against ovarian, breast, and lung cancers, and Kaposi's sarcoma [15]. Unfortunately, when used alone in chemotherapy, it shows serious side-effects such as hypersensitivity, nephrotoxicity, and neurotoxicity [16–20].

Recent studies reported that porphyrin-platinum and porphyrin-cyclodextrin-taxol conjugates exhibit greater antitumor activity and tumor selectivity than parent drugs [20–23]. These studies used porphyrin derivatives to improve the tumor selectivity of the particular anticancer drug. The advantage of the combined therapies is their higher therapeutic effect compared to a single therapy approach [23–25].

Encouraged by these reports, we attempted to conjugate PTX with a well-studied chlorin derivative, pyropheophorbide-a (PPa). In the present study, we describe the synthesis and characterization of the chlorin-based PTX conjugate prepared through the esterification reaction using carbodiimide coupling reagent. In addition, we discuss *in vitro* phototoxicity and darktoxicity of the conjugate against three kinds of cancer cells (HeLa,

\*Correspondence to: Woong Shick Ahn, email: [ahnlab1@catholic.ac.kr](mailto:ahnlab1@catholic.ac.kr), tel: +82 2-2258-6946, fax: +82 2-599-4120

CaSki, and TC-1) as well as their cellular uptake in TC-1 and HeLa cells.

## EXPERIMENTAL

### General

Column chromatographic separations were performed over silica gel 60 (63–200 mesh; Merck, Whitehouse Station, NJ, USA). Analytical thin layer chromatography (TLC) was carried out on precoated sheets with silica gel F254 (0.2 mm thick; Merck,). All reactions were carried out under an argon atmosphere in the dark. The progress of reactions was monitored by TLC and detection was carried out using an ultraviolet-lamp at 265 nm or 365 nm. Electronic absorption and fluorescence spectra were recorded on an Ultrospec<sup>®</sup>3000 spectrophotometer (Pharmacia Biotech, Cambridge, England) and a RF-5301 spectrofluorophotometer (Shimadzu, Japan). Proton nuclear magnetic resonance (<sup>1</sup>H NMR) spectra were recorded on a Unity Inova 500 (UI 500, Varian, Palo Alto, CA, USA) spectrometer at 500 MHz; chemical shifts are expressed in parts per million (ppm) relative to tetramethylsilane (TMS, 0.00). Elemental analysis and matrix-assisted laser desorption/ionization (MALDI) mass spectra were obtained on an EA1112 elemental analyzer and a Voyager-DE<sup>™</sup> STR Biospectrometry Workstation (Applied Biosystems, Carlsbad, CA, USA) spectrometer. High performance liquid chromatography (HPLC) spectra were recorded at 660 nm on an Ultimate 3000 (Dionex, Pittsburgh, PA, USA). Confocal laser microscopy was conducted using a model TCS SP2 apparatus (Leica, Jena, Germany) at 570 nm. All reagents were purchased from Sigma-Aldrich (St. Louis, MO, USA), Fluka (St. Louis, MO, USA), Alfa Aesar (Ward Hill, MA, USA), and Daihan (Seoul, Korea). If necessary, anhydrous solvents were distilled according to standard procedures [26]. Other commercially available reagents were used without further purification. PPa was prepared from methyl pyropheophorbide-a (MPPa), which was obtained *via* methyl pheophorbide-a (MPa) from *Spirulina maxima* algae according to previously reported methods [27, 28]. We prepared PPa using a previously reported procedure [29]. Yield 1.0 g (88.5%). Rf: 0.25 (5% methanol in dichloromethane). UV-vis (CH<sub>2</sub>Cl<sub>2</sub>): λ<sub>max</sub>, nm (M<sup>-1</sup>.cm<sup>-1</sup>) 667.7 (43162.1), 414.2 (80694.4). <sup>1</sup>H NMR spectrum of PPa was interpreted as similar with previously reported in [27, 28]. Proton signals in <sup>1</sup>H NMR spectrum for neat Paclitaxel were consistent to those reported in [30].

### Synthesis of pyropheophorbide-a-paclitaxel (PPa-PTX) conjugate

PPa (14.41 mg, 0.026 mmol), paclitaxel (23 mg, 0.026 mmol), *N,N'*-dicyclohexylcarbodiimide (DCC; 11.12 mg, 0.053 mmol), and dimethylaminopyridine

(DMAP; 3.3 mg, 0.028 mmol) were dissolved in anhydrous dichloromethane (4 mL). Next, the reaction mixture was stirred under argon at room temperature in the dark for 6 h. Progress of the reaction was monitored by TLC using 2% methanol in dichloromethane until the starting material was completely consumed. Then, 50 mL of dichloromethane and 100 mL of water were added to the reaction mixture and the organic layer was washed with water, 5% hydrochloric acid solution, and a saturated solution of sodium chloride. The organic layer was then dried over anhydrous sodium sulfate. To remove the byproduct dicyclohexylurea (DCU) formed from DCC, the residue was dissolved in ethyl acetate and filtered by suction. After that, the solvent was removed under vacuum and the residue was purified on silica gel (230–400 mesh) and eluted with 10% acetone in dichloromethane to produce the target compound. Finally, the product was recrystallized from dichloromethane-hexane. Yield 29.0 mg (81.5%); brown-grey solid; Rf: 0.27 (2% methanol in dichloromethane). Anal. calcd. for C<sub>80</sub>H<sub>83</sub>O<sub>16</sub>N<sub>5</sub>: C, 70.11; H, 6.10; N, 5.11. Found: C, 70.30; H, 6.11; N, 5.18. UV-vis (CH<sub>2</sub>Cl<sub>2</sub>): λ<sub>max</sub>, nm (M<sup>-1</sup>.cm<sup>-1</sup>) 667.6 (38291.6), 414.1 (75350.2). <sup>1</sup>H NMR (500 MHz; CDCl<sub>3</sub>; Me<sub>4</sub>Si): δ<sub>H</sub>, ppm (ppa stands for pyropheophorbide-a and tax stands for paclitaxel) 9.48 (s, 1H, 10-*meso*-H<sub>ppa</sub>), 9.39 (1H, s, 5-*meso*-H<sub>ppa</sub>), 8.52 (1H, s, 20-*meso*-H<sub>ppa</sub>), 8.1 (2H, d, 23-, 27-CH<sub>tax</sub>, *J* = 7.02 Hz), 8.01 (1H, dd, 3'-CH<sub>ppa</sub>, *J* = 11.5, 17.8 Hz), 7.64 (2H, d, 39-, 43-CH<sub>tax</sub>, *J* = 7.4 Hz), 7.4 (4H, m, 25-, 24-, 26-, and 41-CH<sub>tax</sub>), 7.3 (2H, d, 33-, 37-CH<sub>tax</sub>, *J* = 4.2 Hz), 7.24 (5H, m, 40-, 42-, 34-, 36-, and 35-CH<sub>tax</sub>), 6.8 (1H, d, 4'NH<sub>tax</sub>, *J* = 6.7 Hz), 6.28 (1H, s, 10-CH<sub>tax</sub>), 6.23 (2H, dd, 3<sup>2</sup>-CH<sub>2ppa</sub>, *J* = 17.9, 11.5 Hz), 6.22 (1H, t, 13-CH<sub>tax</sub>, *J* = 8.9 Hz), 5.94 (1H, m, 3'CH<sub>tax</sub>), 5.67 (1H, d, 2-C<sub>tax</sub>, *J* = 7 Hz), 5.58 (1H, d, 2'CH<sub>tax</sub>, *J* = 2.6 Hz), 5.11 (2H, dd, 13<sup>2</sup>-CH<sub>2ppa</sub>, *J* = 19.5, 19.5 Hz), 4.95 (1H, d, 5-CH<sub>tax</sub>, *J* = 7.4 Hz), 4.43 (2H, m, 18-CH<sub>ppa</sub> and 7-CH<sub>tax</sub>, overlapped), 4.27 (2H, m, 7-CH<sub>ppa</sub>, 20<sup>a</sup>-CH<sub>tax</sub> overlapped), 4.18 (1H, d, 20<sup>b</sup>-CH<sub>tax</sub>, *J* = 8.5 Hz), 3.79 (1H, d, 3-CH<sub>tax</sub>, *J* = 7 Hz), 3.69 (2H, q, 8<sup>1</sup>-CH<sub>2ppa</sub>, *J* = 7.5 Hz), 3.62 (3H, s, 12<sup>1</sup>-CH<sub>3ppa</sub>), 3.40 (3H, s, 2<sup>1</sup>-CH<sub>3ppa</sub>), 3.24 (3H, s, 7<sup>1</sup>-CH<sub>3ppa</sub>), 2.61 (2H, m, 17<sup>2</sup>-CH<sub>2ppa</sub>), 2.56 (1H, s, 7-OH<sub>tax</sub>), 2.5 (1H, m, 6<sup>a</sup>-CH<sub>tax</sub>), 2.41 (3H, s, 29-CH<sub>3tax</sub>), 2.36 and 2.13 (4H, m, 4-CH<sub>2tax</sub>, 17<sup>1</sup>-CH<sub>2ppa</sub>, overlapped), 2.21 (3H, s, 31-CH<sub>3tax</sub>), 1.92 (3H, s, 19-CH<sub>3tax</sub>), 1.88 (1H, s, 1-OH<sub>tax</sub>), 1.85 (1H, m, 6<sup>b</sup>-CH<sub>tax</sub>), 1.75 (3H, d, 18<sup>1</sup>-CH<sub>3ppa</sub>, *J* = 7.3 Hz), 1.69 (3H, t, 8<sup>2</sup>-CH<sub>3ppa</sub>, *J* = 7.5 Hz), 1.68 (3H, s, 18-CH<sub>3tax</sub>), 1.21 (3H, s, 17-CH<sub>3tax</sub>), 1.12 (3H, s, 16-CH<sub>3tax</sub>), 0.48 (1H, brs, 21-NH<sub>ppa</sub>), -1.67 (1H, brs, 23-NH<sub>ppa</sub>). <sup>13</sup>C NMR (500 MHz; CDCl<sub>3</sub>): δ<sub>C</sub>, ppm 204.03 (s, C<sub>9tax</sub>), 196.27 (s, 13<sup>1</sup>-C<sub>ppa</sub>), 172.52 (s, 1<sup>1</sup>-C<sub>tax</sub>), 171.41 (s, 17<sup>3</sup>-C<sub>ppa</sub>), 171.38 (s, 30-C<sub>tax</sub>), 170.02 (s, 28-C<sub>tax</sub>), 168.18 (s, 21-C<sub>tax</sub>), 167.2 (s, 5<sup>1</sup>-C<sub>tax</sub>), 159.93 (s, 19-C<sub>ppa</sub>), 155.61 (s, 16-C<sub>ppa</sub>), 151.11 (s, 6-C<sub>ppa</sub>), 149.22 (s, 9-C<sub>ppa</sub>), 1.37 (s, 14-C<sub>ppa</sub>), 142.82 (s, 8-C<sub>ppa</sub>), 141.83 (s, 1-C<sub>ppa</sub>), 138.12 (s, 11-C<sub>ppa</sub>), 137.01 (s, 12-C<sub>tax</sub>), 136.51 (s, 3-C<sub>ppa</sub>), 136.42 (s, 4-C<sub>ppa</sub>), 136.22 (s, 7-C<sub>ppa</sub>), 133.75 (s, 25-C<sub>tax</sub>), 133.71 (s, 32-C<sub>tax</sub>), 133.09

(s, 11-C<sub>tax</sub>), 132.16 (s, 41-C<sub>tax</sub>), 131.82 (s, 2-C<sub>ppa</sub>), 130.67 (s, 12-C<sub>ppa</sub>), 130.37 (s, 23, 27-C<sub>tax</sub>), 129.46 (s, 22-C<sub>tax</sub>), 129.40 (s, 31-C<sub>ppa</sub>), 129.26 (s, 34, 36-C<sub>tax</sub>), 128.90 (s, 24, 26, 40, 42-C<sub>tax</sub>), 128.86 (s, 13-C<sub>ppa</sub>), 128.66 (s, 35-C<sub>tax</sub>), 127.22 (s, 33, 37-C<sub>tax</sub>), 126.7 (s, 39, 43-C<sub>tax</sub>), 122.9 (s, 32-C<sub>ppa</sub>), 106.14 (s, 15-C<sub>ppa</sub>), 104.47 (s, 10-C<sub>ppa</sub>), 97.56 (s, 20-C<sub>ppa</sub>), 84.69 (s, 5-C<sub>tax</sub>), 81.30 (s, 4-C<sub>tax</sub>), 79.38 (s, 1-C<sub>tax</sub>), 76.66 (s, 20-C<sub>tax</sub>), 75.81 (s, 10-C<sub>tax</sub>), 75.36 (s, 2-C<sub>tax</sub>), 74.37 (s, 2'-C<sub>tax</sub>), 72.32 (s, 13-C<sub>tax</sub>), 72.15 (s, 7-C<sub>tax</sub>), 58.74 (s, 8-C<sub>tax</sub>), 53 (s, 3'-C<sub>tax</sub>), 51.62 (s, 17-C<sub>ppa</sub>), 50.1 (s, 18-C<sub>ppa</sub>), 48.23 (s, 13<sup>2</sup>-C<sub>ppa</sub>), 45.83 (s, 3-C<sub>tax</sub>), 43.4 (s, 15-C<sub>tax</sub>), 35.86 (s, 6-C<sub>tax</sub>), 35.77 (s, 14-C<sub>tax</sub>), 30.77 (s, 17<sup>1</sup>-C<sub>ppa</sub>), 29.9 (s, 17<sup>2</sup>-C<sub>ppa</sub>), 27.04 (s, 17-C<sub>tax</sub>), 23.26 (s, 18<sup>1</sup>-C<sub>ppa</sub>), 22.87 (s, 29-C<sub>tax</sub>), 22.37 (s, 16-C<sub>tax</sub>), 21.03 (s, 31-C<sub>tax</sub>), 19.7 (s, 8<sup>1</sup>-C<sub>ppa</sub>), 17.6 (s, 8<sup>2</sup>-C<sub>ppa</sub>), 15.06 (s, 18-C<sub>tax</sub>), 12.32 (s, 12<sup>1</sup>-C<sub>ppa</sub>), 12.25 (s, 2<sup>1</sup>-C<sub>ppa</sub>), 11.48 (s, 7<sup>1</sup>-C<sub>ppa</sub>), 9.83 (s, 17-C<sub>tax</sub>). MALDI-MS: *m/z* 1370.5734 (calcd. for [M + H]<sup>+</sup> 1370.5835).

### Singlet oxygen quantum (SOQ) yields

SOQ yields were measured by using previously described techniques in [31, 32]. The SOQ yield ( $\phi_{\Delta}$ ) of each sample was calculated from standard  $\phi_{\Delta}$  value (PPa - 0.52) [33].

### MTT assay

TC-1, positive for HPV E6/E7, HeLa (human cervix carcinoma cell), and CaSki (a new epidermoid cervical cancer cell) cell lines were used. For viable cell counting, the cells ( $3 \times 10^3$  cells) per well (96 well plate) were treated with PPa, PPa-PTX conjugate, or PTX at 0.03, 0.06, 0.125, 0.25, 0.5, 1 and 2  $\mu\text{M}$  after incubation for 24 h (37 °C, 5% CO<sub>2</sub>) in RPMI 1640 containing 5% fetal bovine serum (FBS). After the cells were incubated for 24 h, laser irradiation ( $662 \pm 3$  nm, 6.25 J/cm<sup>2</sup>) was performed and the other sample was kept in dark. Cell growth inhibition was determined a 3-(4,5-dimethylthiazol-2-yl)-2,5-diphenyltetrazolium bromide (MTT)-based assay 24 h after irradiation. For the MTT assay, 20  $\mu\text{L}$  of 5 mg/mL MTT solution was added to each cell culture well and cultured for 4 h. Next, 100  $\mu\text{L}$  of dimethylsulfoxide was added to the culture, shaken for 10 sec, and the absorbance was measured with a Spectra Max 340 ELISA reader (Molecular Devices, Sunnyvale, CA, USA) at 570 nm. Measurements were performed 24 h after laser irradiation. Each group consisted of three wells; the means of their values were used as the measured values. The mean  $\pm$ SD values were used for the expression of data.

### Cellular uptake

The cells ( $5 \times 10^4$ ) in RPMI-1640 (2 mL) with 10% FBS were seeded into each well of 6-well plate on coverslips and incubated at 37 °C in a humidified atmosphere of 5% CO<sub>2</sub> for 24 h. Fresh medium containing 2  $\mu\text{M}$  PPa or PPa-PTX was added, and cells were incubated for various time

points (0.5, 1, 2, 3, 6, 9, 12, 24, 48, and 72 h). The cells were then washed twice with phosphate buffered saline (PBS) buffer and stained with 30  $\mu\text{M}$  4',6'-diamino-2-phenylindole (DAPI) solution (500  $\mu\text{L}$ /well) for 10 min at 37 °C. After that, 1 mL of paraformaldehyde (PFA, 1%) was loaded into each well of 6-well plates for fixation of cells. After 15 min, the supernatant was discarded and the coverslip holding cells were put a slide glass where a drop of mounting solution was placed. After drying for 4 h at room temperature, fluorescence was visualized using a model TCS SP2 Laser Scanning Spectral Confocal Microscope (Leica). Fluorescence images were taken at emission wavelengths of 545 nm and 675 nm. Images of PPa and PPa-PTX conjugate were assigned as red color.

## RESULTS AND DISCUSSION

### Synthesis and characterization

As shown in Fig. 1, we synthesized the PPa-PTX conjugate with the intention of searching an optimal anticancer agent for cancer treatment. Antitumor active PTX contains three hydroxyl groups at 2', 1- and 7-positions, and the hydroxyl group at the 2' position displays higher reactivity than the others [5–8, 34]. Therefore, to synthesize the target PPa-PTX conjugate, we linked the hydroxyl group at the 2' position of the PTX moiety and the carboxyl group at the 17<sup>3</sup> position of the PPa moiety through an ester bond. Reaction of PPa with commercial PTX using DCC as a coupling reagent in the presence of DMAP at room temperature in the absence of light produced high yields of the target PPa-PTX conjugate.

Subsequently, the structure of PPa-PTX (Fig. 1) was fully characterized by <sup>1</sup>H NMR, 2D <sup>1</sup>H-<sup>1</sup>H COSY, <sup>1</sup>H-<sup>13</sup>C HSQC and <sup>13</sup>C NMR techniques, as well as by MALDI-time of flight-mass spectrometry, UV-vis and fluorescence spectroscopy, and HPLC.

Figure 2 shows the <sup>1</sup>H NMR spectra of neat PTX and PPa-PTX. After the synthesis of the target compound, the position of an ester bond bridging PPa and PTX can be determined as the absence of a resonance corresponding to either of hydroxyl groups of the PTX moiety for the <sup>1</sup>H NMR spectrum of the final PPa-PTX conjugate. Based on this, compared to the <sup>1</sup>H NMR spectrum of PTX, the spectrum of PPa-PTX did not show a resonance of the hydroxyl group at the C2' that appeared at 3.50 ppm in the <sup>1</sup>H NMR spectrum of neat PTX. The signals of protons at the C2' and C3' positions neighboring the 2'OH group for the PTX moiety shifted downfield (0.79 and 0.15 ppm, respectively) because of a newly formed ester bond in PPa-PTX. Moreover, a proton (at 2.56 ppm) at the 7-OH position was determined to be unreacted. A proton signal of the 1-OH group clearly appeared at corresponding position (at 1.87 ppm). Multiplets (at 4.43, 2.36 and 2.13 ppm) were observed as overlapping proton

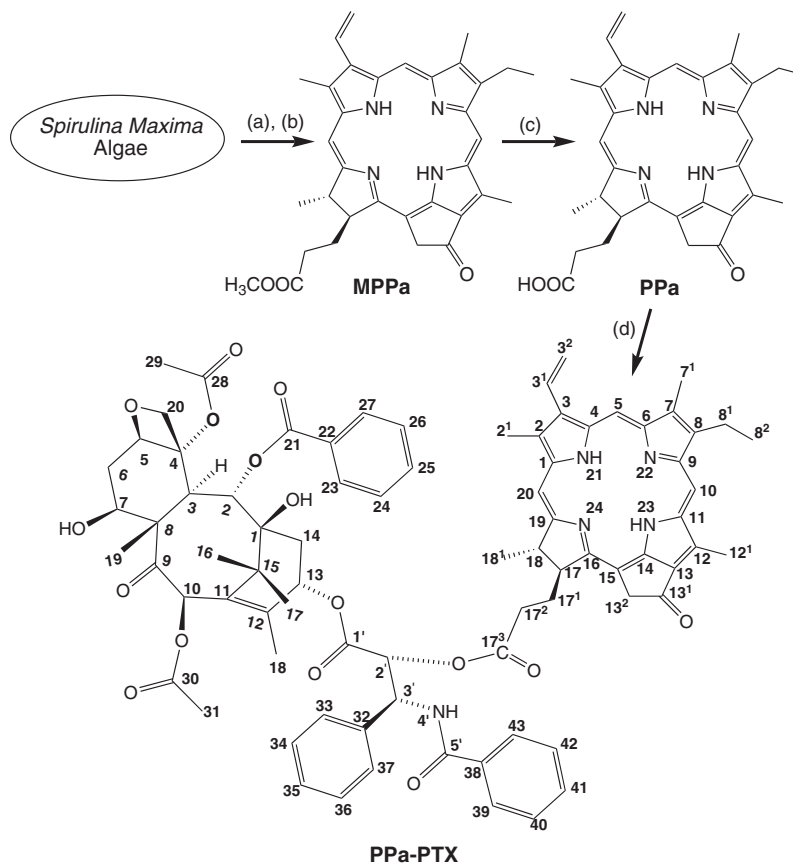


**Fig. 1.** Synthesis of pyropheophorbide-a-paclitaxel conjugate. Reagents and conditions: (a) Extraction and acidic treatment; (b) Methylpheophorbide-a, reflux in collidine for 1.5 h; (c) Acidic treatment with 50%  $\text{H}_2\text{SO}_4$  for 2 h at room temperature; (d) Paclitaxel, DMAP and DCC in dichloromethane at room temperature for 6 h

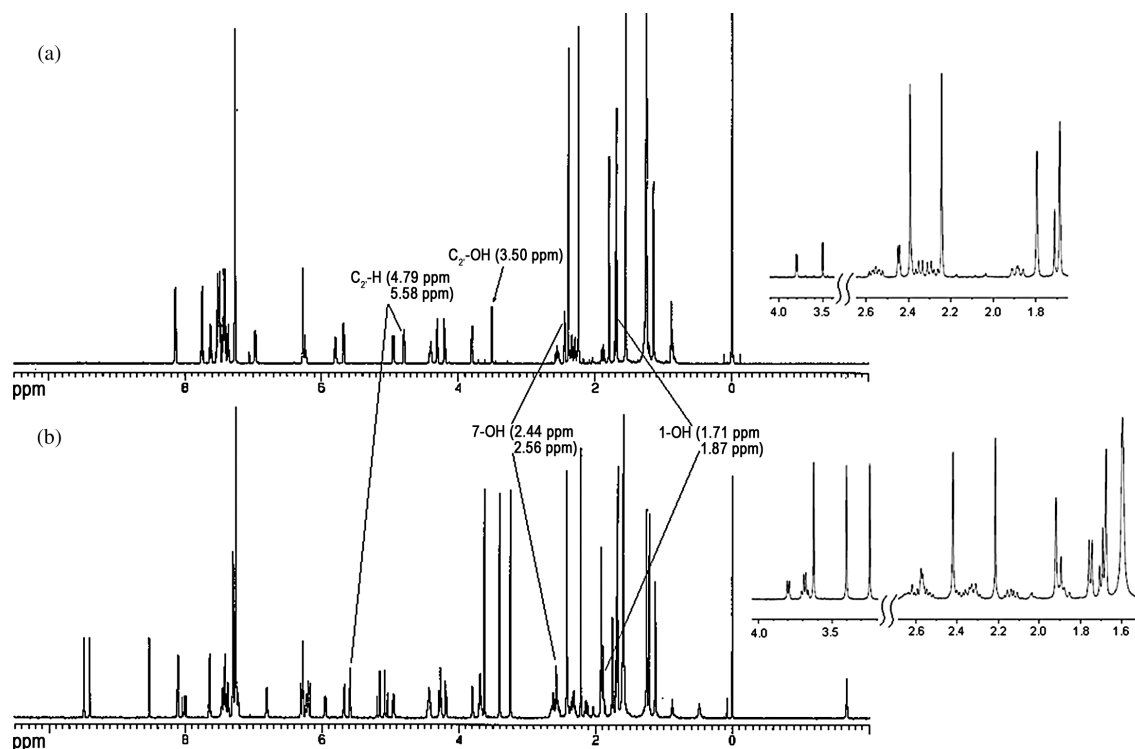


**Fig. 2.** Comparison of  $^1\text{H}$  NMR spectra of PTX and PPa-PTX. (a)  $^1\text{H}$  NMR spectrum of PTX in  $\text{CDCl}_3$ ; (b)  $^1\text{H}$  NMR spectrum of PPa-PTX conjugate in  $\text{CDCl}_3$

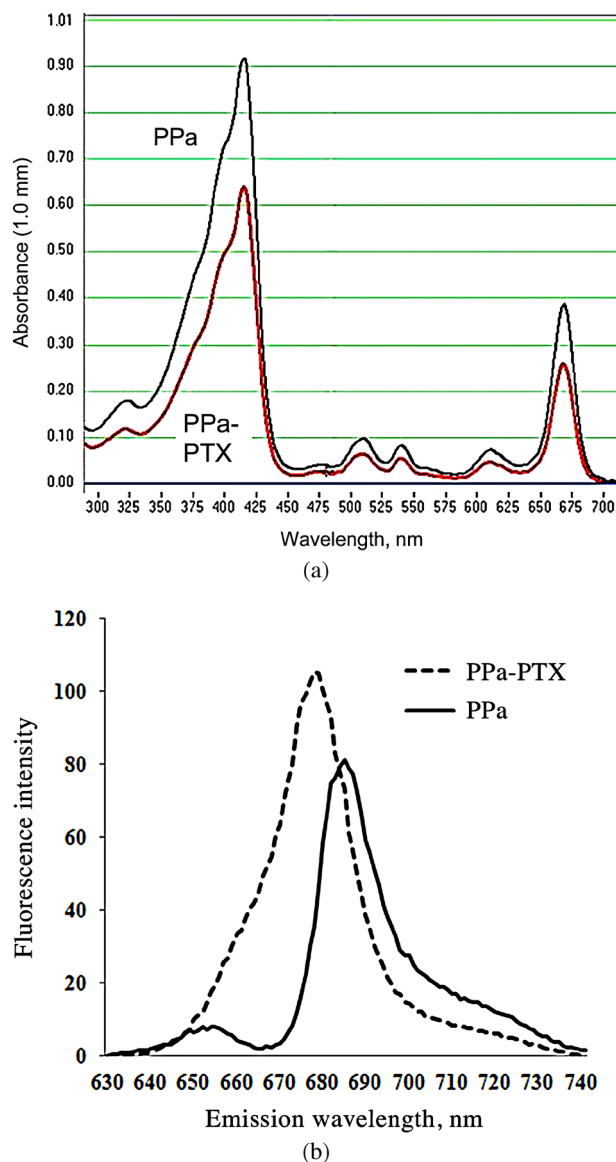


**Fig. 3.** UV absorption (a) and fluorescence emission (b) spectra of PPa and PPa-PTX conjugate in DMSO and DMF at same concentration (1  $\mu\text{M}$ )

signals at C18 and C17<sup>1</sup> positions of the PPa moiety with protons at C7 and C14 positions of the PTX moiety. The proton NMR spectrum demonstrated that an ester bond formed at 2' position for the PTX moiety. The other peaks of PPa and PTX moieties of PPa-PTX in the NMR spectrum revealed no significant difference and were easy to produce assignments for. The <sup>13</sup>C NMR spectrum of PPa-PTX was fully cleared up and the carbon atoms of the PTX moiety were assigned using data previously reported [30, 35].

The MALDI-TOF mass spectrum of PPa-PTX showed a peak at  $m/z = 1370.5734$  (100%) for its molecular ion. The purity of PPa-PTX was determined to be 99.45% by the analytical reversed-phase HPLC at 660 nm using methanol/acetone (95:5) as an eluent.

The UV absorption and fluorescence spectra of PPa and PPa-PTX in dimethylsulfoxide (DMSO) were determined to observe differences by spectrophotometry.

There were no significant differences between the UV absorption spectra of PPa and PPa-PTX, as shown in Fig. 3a, but a slightly reduced extinction coefficient was observed in case of PPa-PTX. This may have been influenced *via* the PTX moiety in conjugate. There was no absorption for the phenyl groups from the PTX moiety of PPa-PTX.

As illustrated in Fig. 3b, conjugation of PPa and PTX led to a slight blue shift from 685 nm to 679 nm, and a noticeable increase in the fluorescence intensity of PPa-PTX.

### Singlet oxygen quantum yield

To determine whether the conjugate is a potential candidate as a PS in PDT, an indirect method [35] was utilized to detect a decrease of fluorescence emission intensity for 9,10-dimethylanthracene (DMA), which can react with singlet oxygen produced from PS when irradiation was given. The singlet oxygen yield of the conjugate was calculated 0.42 which was little bit lower than that (0.52) of PPa.

### Phototoxicity and darktoxicity

We performed an *in vitro* assay of cell viability on HeLa, CaSki, and TC-1 cancer cell lines to examine the phototoxicity and darktoxicity effects of the PPa-PTX conjugate. The cells ( $3 \times 10^3$  cells/well) were incubated with PPa, PPa-PTX, or PTX for 24 h, and photoirradiated with a predetermined light dose ( $662 \pm 3$  nm,  $6.25 \text{ J/cm}^2$ ). Viability of the cells treated with PPa, PPa-PTX conjugate, or PTX at various concentrations (0.01, 0.03, 0.06, 0.12, 0.25, 0.5, 1, and 2  $\mu\text{M}$ ) was determined at 24 h with and without irradiation as described before [36].

Figure 4 shows the results of phototoxicity and darktoxicity of PPa, PTX, and PPa-PTX conjugate at the various concentrations against HeLa, CaSki, and TC-1 cells. The phototoxicity results of the agents at 0.01–0.25  $\mu\text{M}$  are illustrated.

In case of HeLa cell line (Fig. 4a), PPa-PTX conjugate at 0.01–0.06  $\mu\text{M}$  produced 50%–20% cell viability, whereas PPa at the same concentrations produced around 100%–60% cell viability. These results indicate that the PPa-PTX conjugate has more than double the phototoxic effect compared to PPa. However, PPa at a higher concentration (0.12  $\mu\text{M}$ ) was completely toxic, with no cell survival, which exceeded that of PPa-PTX. In the darktoxicity test, PPa, PPa-PTX, and PTX showed negligible effects.

In case of CaSki cells (Fig. 4b), PPa-PTX at 0.01–0.06  $\mu\text{M}$  showed 80%–60% cell viability, while PPa at the same concentrations produced 100%–95% cell viability. These results also confirmed that the conjugate had

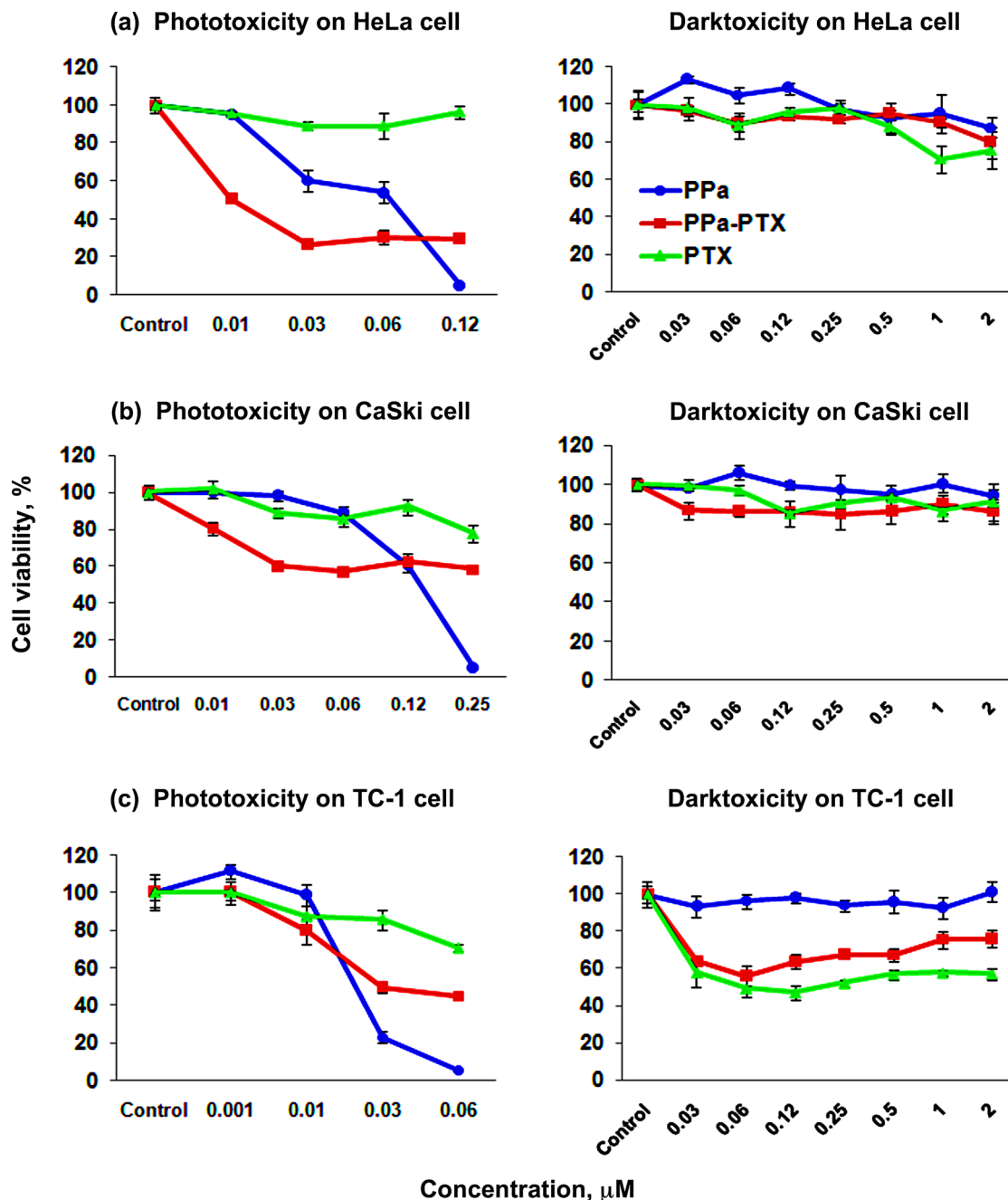


**Fig. 4.** Comparison of results of PDT and darktoxicity of PPa, PTX and PPa-PTX conjugate at various concentration range (0.03–2  $\mu\text{M}$ ) in three cell lines; HeLa (a), CaSki (b) and TC-1 (c). Cells were incubated with PS or PTX in 10% serum containing medium for 24 h and then exposed to light (662.5 nm) for a total fluence of 6.25  $\text{J}/\text{cm}^2$ . In case of darktoxicity, irradiation was not given. After treatment, the cells were incubated in growth medium for 24 h. The data are expressed as mean of three experiments. Error bars present standard deviation

20%–40% higher phototoxicity than free PPa at same condition. PPa at 0.25  $\mu\text{M}$  produced no cell viability. In the darktoxicity test, PPa, PPa-PTX, and PTX showed negligible effects.

In case of the TC-1 cell line (Fig. 4c), PPa-PTX conjugate at 0.01–0.06  $\mu\text{M}$  produced 80%–40% cell viability, while PPa at the same concentrations produced 100%–0% cell viability. The data indicated that the conjugate had a lower phototoxicity, except 0.01  $\mu\text{M}$ , than free PPa in this cell

line. In the darktoxicity test, PPa-PTX showed similar cytotoxicity with PTX at all concentrations.

The three cell lines were affected differently by free PPa and PPa-PTX when irradiated. HeLa and CaSki cells were 30%–40% more sensitive for PPa-PTX at 0.01–0.06  $\mu\text{M}$  than free PPa, whereas, TC-1 cells were more sensitive to free PPa than the others. As reported [37–39], free PPa is 100% phototoxic at concentrations exceeding 0.15  $\mu\text{M}$  in several cancer cell lines, when the same

laser power was used. In addition, some pheophorbide-a derivatives are 50% phototoxic in different cell lines at 0.07–1.5  $\mu\text{M}$  [40–42].

The results indicate some improvements using the PPa-PTX conjugate, especially in HeLa and CaSki cell lines. This enhancement might be related to a combination of PS and anticancer drug.

### Cellular uptake

As shown in Fig. 5, the cellular uptake of PPa and PPa-PTX (2  $\mu\text{M}$ ) in the presence of DAPI in TC-1 (Fig. 5a) and HeLa (Fig. 5b) cells at different time points (0.5, 1, 2, 3, 6, 9, 12, 24, 48, and 72 h) was examined to observe time-dependent penetration of the conjugate into the cells

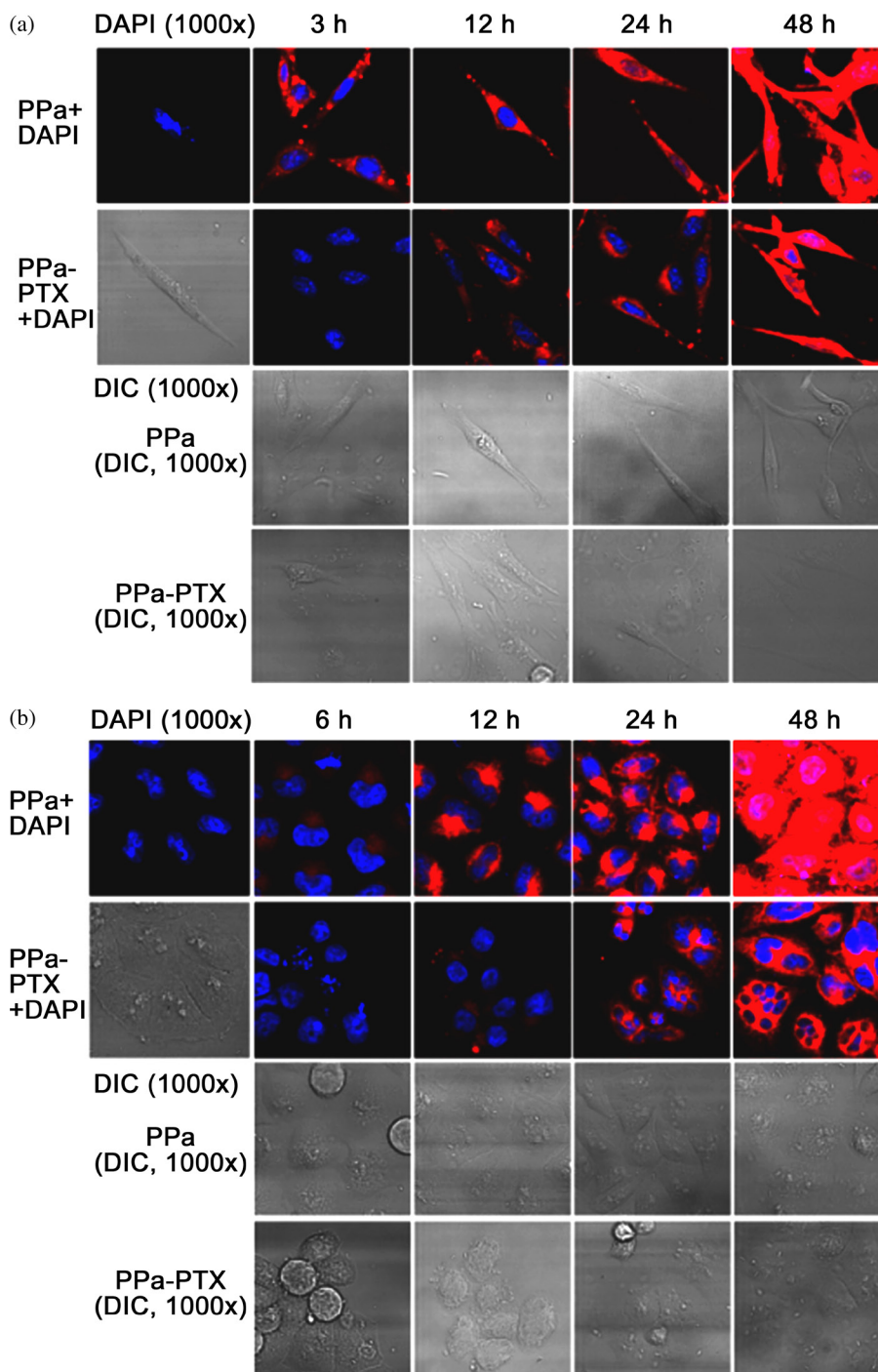


**Fig. 5.** Comparison of cellular uptake results (1000  $\times$ ) for 2  $\mu\text{M}$  of free PPa and PPa-PTX conjugate in TC-1 cells (a) and HeLa cells (b) after different points of time (3, 6, 12, 24, and 48 h) by confocal microscopy. DAPI, which gives blue fluorescence, was used as a staining probe for cell nucleus. Differential interference contrast (DIC) denotes a picture was taken without fluorescence. Red fluorescence refers to presence of PS

by confocal microscopy. Here, we have chosen images of cells treated with PPa and PPa-PTX taken after 3, 6, 12, 24, and 48 h of incubation.

The results confirmed that the uptake of PPa-PTX into TC-1 cell began after 6 h incubation, whereas the uptake of PPa started later, at 3 h incubation (Fig. 5a). Moreover, in case of HeLa cell, uptake of PPa-PTX conjugate began after 9 h incubation, while uptake of PPa started after 6 h of incubation (Fig. 5b). The uptake of PPa and PPa-PTX in HeLa cells was slightly slower than that in TC-1 cells. However, maximum uptake occurred in both cells 24 h after adding PS. The collective observations support the view that both PPa and PPa-PTX had completely entered the cells by 24 h. The late uptake of the PPa-PTX conjugate could be related to the bigger structure of this molecule, which could influence its transport through the cell membrane.

In summary, we have synthesized and characterized a novel PPa-PTX conjugate. Its phototoxicity and darktoxicity were evaluated on three kinds of cancer cell lines (HeLa, CaSki, and TC-1) by an established MTT assay. PPa-PTX at lower concentrations (0.01–0.06  $\mu\text{M}$ ) displayed better phototoxicity in HeLa and CaSki cell lines compared to PPa. Cellular uptake of the conjugate and PPa was also examined in HeLa and TC-1 cells; PPa-PTX conjugate fully entered the cells within 24 h. Further studies will focus on the cellular localization of PPa and PPa-PTX to test whether the efficacy difference relates to PS localization in the cells, and whether the higher phototoxicity of the conjugate at lower dosage in HeLa and TC-1 cells is due to the over-expression of the ABCG2 protein. As well, *in vivo* experiments will be conducted to address the hypothesis that the conjugate may show more phototoxicity even at higher dosage than PPa because there is a fact that *in vitro* efficacy of PPa derivatives reduces for *in vivo* test [43].

### Acknowledgements

The study was supported by The Catholic Harvard Wellman Photomedicine Core Technique Development Center funded by the Ministry of Education, Science and Technology, Seoul, Republic of Korea (Grant No. 5-2012-A0154-00001). The funders had no role in study design, data collection and analysis, decision to publish, or preparation of the manuscript.

### REFERENCES

- Dougherty TJ, Gomer CJ, Henderson BW, Jori G, Kessel D, Korbelik M, Moan J and Peng Q. *J. Natl. Cancer Inst.* 1998; **90**: 889–905.
- Sternberg ED, Dolphin D and Brückner C. *Tetrahedron.* 1998; **54**: 4151–4202.
- Dougherty TJ. *J. Clin. Laser. Med. Surg.* 2002; **20**: 3–7.
- Zheng G, Potter WR, Camacho SH, Missert JR, Wang G, Bellnier DA, Henderson BW, Rodgers MAJ, Dougherty TJ and Pandey RK. *J. Med. Chem.* 2001; **44**: 1540–1559.
- Bonnet R. *Chem. Soc. Rev.* 1995; **24**: 19–33.
- Brandis AS, Salomon Y and Scherz A. *Bacteriochlorophyll Sensitizers in Photodynamic Therapy, Chlorophylls and Bacteriochlorophylls: Biochemistry, Biophysics, Functions and Applications*, Grimm B, Porra RJ, Rudiger W and Scheer H. (Eds.) Springer: Dordrecht, 2006; pp 461–494.
- Pandey RK, Sumlin AB, Potter WR, Bellnier DA, Henderson BW, Constantine S, Aoudia M, Rodgers MRJ, Smith KM and Dougherty TJ. *Photochem. Photobiol.* 1996; **63**: 194–205.
- Reshetnickov AV, Babushkina TA, Kirillova GV and Ponomarev GV. *Chem. Heterocycl. Compd.* 2001; **37**: 191–201.
- Borle F, Radu A, Fontollet C, van den Bergh H, Monnier P and Wagnières G. *Br. J. Cancer.* 2003; **89**: 2320–2326.
- Dąbrowski JM, Urbanska K, Arnaut LG, Pereira MM, Abreu AR, Simões S and Stochel G. *ChemMedChem.* 2011; **6**: 465–475.
- Sobolev AS. *Bio Essays.* 2008; **30**: 278–287.
- Taxol.® Science and Application*, Suffness M. (Ed.) CRC Press: Boca Raton, FL, 1995.
- Wani MC, Taylor HL, Wall ME, Coggon P and McPhail AT. *J. Am. Chem. Soc.* 1971; **93**: 2325–2327.
- McGuire WP, Rowinsky EK, Rosenshein NB, Grumbine FC, Ettinger DS, Armstrong DK and Donehower RC. *Ann. Intern. Med.* 1989; **111**: 273–279.
- Bradley MO, Webb NL, Anthony FH, Devanesan P, Witman PA, Hemamalini S, Chander MC, Baker SD, He L, Horwitz SB and Swindell CS. *Clin. Cancer Res.* 2001; **7**: 3229–3238.
- Weiss RB, Donehower RC and Wiernik PH. *J. Clin. Oncol.* 1990; **8**: 1263–1268.
- Zhang W, Junguo H, Shi Y, Yajuan L, Wu J, Xianyi S and Xiaoling F. *Inter. J. Pharm.* 2009; **376**: 176–185.
- Skwarczynski M, Noguchi M, Hirota S, Sohma Y, Kimura T, Hayashi Y and Kiso Y. *Bioorg. Med. Chem. Lett.* 2006; **16**: 4492–4496.
- Li P, Jiang S, Pero SC, Oligino L, Krag DN, Michejda CJ and Roller PP. *Biopolymers.* 2007; **87**: 225–230.
- Brunner H and Schellerer KM. *Inorg. Chim. Acta.* 2003; **350**: 39–48.
- Lottner C, Bart KC, Bernhardt G and Brunner H. *J. Med. Chem.* 2002; **45**: 2064–2078.
- Kim YS, Song R, Kim DH, Jun MJ and Sohn YS. *Bioorg. Med. Chem.* 2003; **11**: 1753–1760.
- Kralova J, Keji k Z, Briza T, Pouckova P, Kral A, Martasek P and Kral V. *J. Med. Chem.* 2010; **53**: 128–138.
- Jeferson AN, Sergio HT, Juliano AB, Koiti A and Henrique ET. *J. Inorg. Biochem.* 2009; **103**: 182–189.

25. Noguchi M, Skwarczynski M, Prakash H, Hirota S, Kimura T, Hayashi Y and Kiso Y. *Bioorg. Med. Chem.* 2008; **16**: 5389–5397.
26. Perkin DD and Armarego WLF. *Purification of Laboratory Chemicals*, Pergamon: Oxford, 1988.
27. Smith KM, Goff DA and Simpson D. *J. Am. Chem. Soc.* 1985; **107**: 4946–4954.
28. Galindev O, Badraa N, Dalantai M, Sengee G, Dorjnamjin D and Shim YK. *Photochem. Photobiol. Sci.* 2008; **7**: 1273–1281.
29. Nifantiev NE and Yashunsky DV. *Water-Soluble Porphyrin Derivatives for Photodynamic Therapy, their use and Manufacture*, In US Patent 6,777,402 B2. CeramOptec Industries, Inc. East Longmeadow, MA, 2004.
30. Chen JZ, Banade SV and Xie XQ. *Inter. J. Pharm.* 2005; **305**: 129–144.
31. Bae BC and Na K. *Biomaterials* 2010; **31**: 6325–6335.
32. Choi Y, McCarthy JR, Weissleder R and Tung C-H. *ChemMedChem* 2006; **1**: 458–463.
33. Al-Omari S and Ali A. *Gen. Physiol. Biophys.* 2009; **28**: 70–77.
34. Lee JW, Lu JY, Low PS and Fuchs PL. *Bioorg. Med. Chem.* 2002; **10**: 2397–2414.
35. Chmurny GN, Hilton BD, Brobst S, Look SA, Witherup KM and Beutler JA. *J. Nat. Prod.* 1992; **55**: 414–423.
36. Wen LY, Bae S-M, Do JH, Park K-S and Ahn WS. *J. Porphyrins Phthalocyanines* 2011; **15**: 174–180.
37. Savellano MD, Pogue BW, Hoopes PJ, Vitetta ES and Paulsen KD. *Cancer Res.* 2005; **65**: 6371–6379.
38. Liu T, Wu LY, Choi JK and Berkman CE. *Prostate* 2009; **69**: 585–594.
39. Fiorenza R, Helmreich M, Molich A, Jux N, Hirsch A, Roder B, Witt C and Bohm F. *J. Photochem. Photobiol. B* 2005; **80**: 1–7.
40. Robey RW, Steadman K, Polgar O and Bates SE. *Canc. Biol. Ther.* 2005; **4**: 187–194.
41. Rapozzi V, Zacchigna M, Biffi S, Garrovo C, Cateni F, Stebel M, Zorzet S, Bonora GM, Drioli S and Xodo LE. *Canc. Biol. Ther.* 2010; **10**: 471–482.
42. Sun X and Leung WN. *Photochem. Photobiol.* 2002; **75**: 644–651.
43. Zheng G, Aoudia M, Lee D, Rodgers MA, Smith KM, Dougherty TJ and Pandey RK. *J. Chem. Soc., Perkin Trans.* 2000; **1**: 3113–3121.